

# **Ionization structure and chemical abundances of the Wolf–Rayet nebula NGC 6888 with integral field spectroscopy**

**A. Fernández-Martín<sup>1,2</sup>, J.M. Vílchez<sup>1</sup>, and E. Pérez Montero<sup>1</sup>**

<sup>1</sup> Instituto de Astrofísica de Andalucía (IAA–CSIC), c/Glorieta de la Astronomía s/n, 18008 Granada, Spain

## **Abstract**

In this work we search for the observational footprints of the interactions between the interstellar medium and stellar winds in the Wolf-Rayet nebula NGC 6888 in order to understand its ionization structure, chemical composition, and kinematics. We collected a set of integral field spectroscopy observations across NGC 6888, obtained with PPAK in the optical range performing both 2D and 1D analyses. Attending to the 2D analysis in the north-east part of the nebula, we generated maps of the extinction structure and electron density. We produced diagnostic diagrams and statistical frequency distributions of the radial velocity. Nine integrated spectra were generated over the whole nebula. We measured line intensities to obtain physical parameters and chemical abundances. We inferred that nearly all the zones present an oxygen abundance slightly below the solar values. The derived N/H appears enhanced up to a factor of 6. Helium presents an enrichment in most of the integrated zones, too. Finally, we proposed a scheme of irregular and/or broken shells for NGC 6888 to explain the features observed.

## **1 Introduction**

NGC 6888 (S105) is a proto-typical wind-blown bubble (WBB) associated with the WN6 star WR 136 (HD 192163) [5]. The ellipsoidal shell appears to be geometrically prolate and to have a highly filamentary structure [6]. The expansion velocity of the shell varies in the range 55 – 110 km s<sup>-1</sup> [6, 7]. Spectroscopy of the nebular shell shows that the ionized gas is enriched with N and He, and is slightly underabundant in oxygen [3]. NGC 6888 was the first WBB that has been detected in X-rays [2]. Later X-ray observations detected a filamentary

---

<sup>2</sup>e-mail: alba@iaa.es

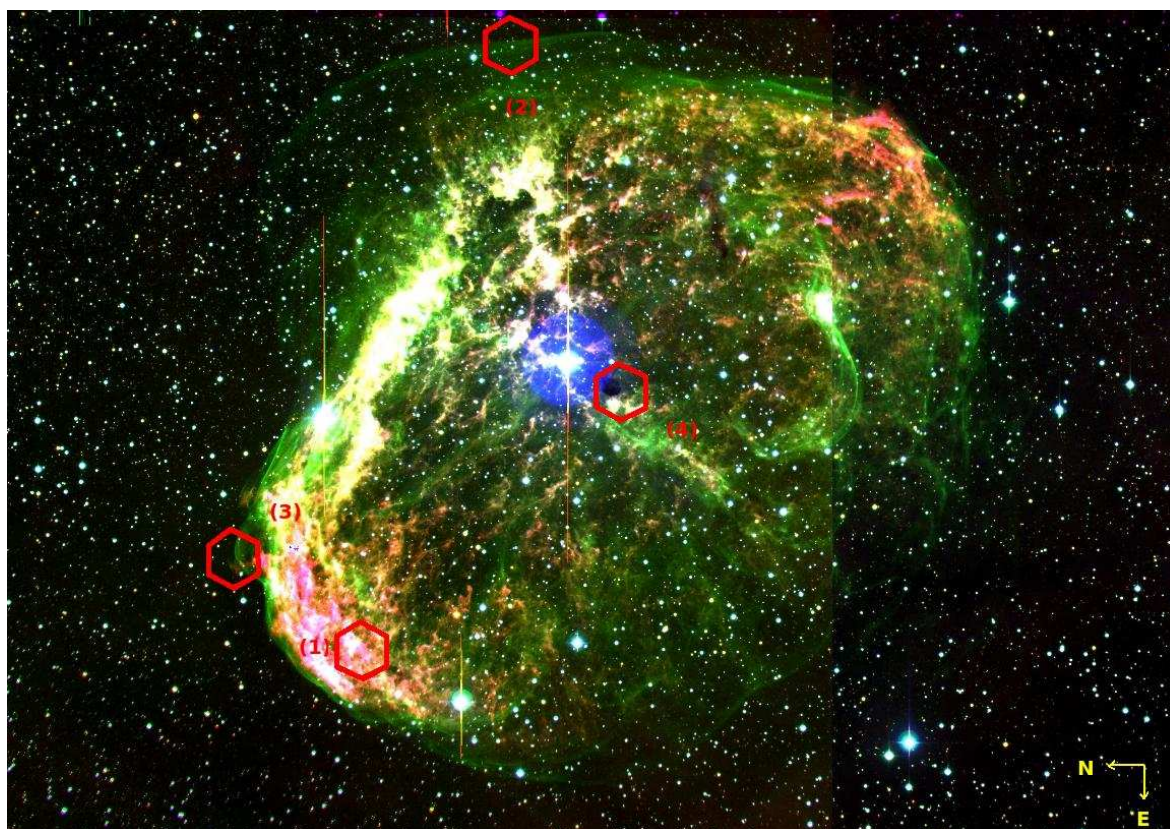


Figure 1: RGB composited image of NGC 6888 taken with the Wide Field Camera at the Isaac Newton Telescope. Red corresponds to the  $H\alpha$  emission, green to  $[OIII]$ , and blue to  $[OII]$ . Red hexagons show the zones of our PPAK observations. North is left and east to the bottom.

structure following the  $H\alpha$  features of the nebula [11] .

## 2 Observations

Basing on the narrow band images observed by our group at the Isaac Newton Telescope (Fig. 1), we chose four zones of NGC 6888 to be observed at the 3.5-m telescope of CAHA (Calar Alto, Almería, Spain) with the Potsdam Multi-Aperture Spectrograph instrument (PMAS) in PPAK mode. We called the observed regions : X-ray zone (1), Edge (2), Mini-bubble (3), and Bullet (4). We used three different gratings to obtain information for the most important emission lines in the optical spectral range. Moreover, in the X-ray zone, we adopted a dithering scheme to fill up gaps between fibres. The data were reduced using the R3D software [9] in combination with the Euro3D packages [8] and IRAF.

### 3 Results

#### 3.1 Two-dimensional study

To analyse the morphology and ionization structure of NGC 6888 we generated interpolated images of the observed regions in three wavelength ranges including the lines  $[\text{OII}]\lambda 3728\text{\AA}$ ,  $[\text{OIII}]\lambda 5007\text{\AA}$ , and  $\text{H}\alpha$  (Fig. 2, left panel).

In the X-ray region (zone (1) in Figs.1 and 2) a dithering scheme was performed, and it was studied in detail by means of the creation of datacubes. We generated several maps: reddening coefficient map,  $c(\text{H}\beta)$ , from the  $\text{H}\alpha/\text{H}\beta$  line ratio (Fig. 2, a in right panel); electron density map,  $n_e$ , from the  $[\text{SII}]\lambda\lambda 6717/6731\text{\AA}$  line ratio (Fig. 2, b in right panel), and radial velocity map from the  $\text{H}\alpha$  emission line (Fig. 2, c in right panel).

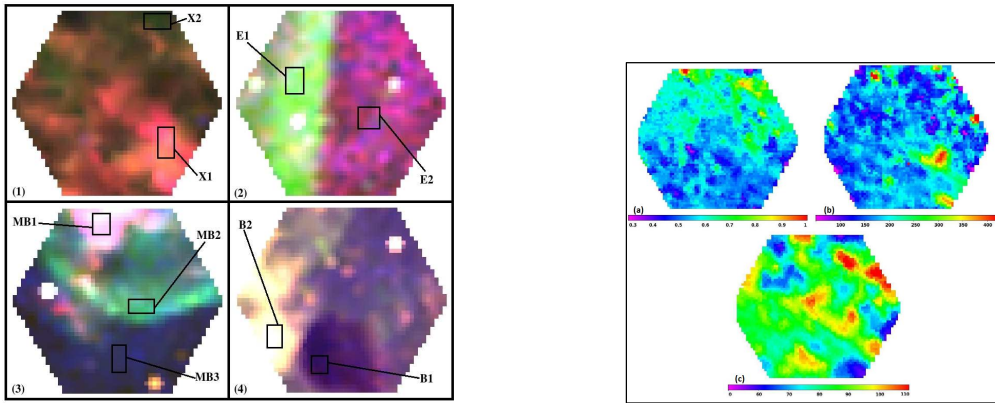


Figure 2: *Left panel:* Interpolated maps of the observed areas. Colours as in Fig. 1. Boxes show regions where the integrated spectra were created. *Right panel* Maps created in the X-ray zone: (a) reddening coefficient map, (b) electron density map in  $\text{cm}^{-3}$ , and (c) radial velocity map for  $\text{H}\alpha$  in  $\text{km s}^{-1}$ .

We generated three diagnostic diagrams:  $[\text{NII}]\lambda 6584/\text{H}\alpha$  vs  $[\text{SII}]\lambda 6731/\text{H}\alpha$ ,  $[\text{OIII}]\lambda 5007/\text{H}\beta$  vs  $[\text{SII}]\lambda 6731/\text{H}\alpha$ , and  $[\text{OIII}]\lambda 5007/\text{H}\beta$  vs  $[\text{NII}]\lambda 6584/\text{H}\alpha$ . A reference fit was performed in the first diagram locating in a map spaxels inside/outside the nominal limits of  $3\sigma$ . We found that points with a similar tendency in the BPT appear grouped in the PPAK FoV. Attending to these results we defined three zones: *Zone A* with correlations between lines and with the maximum emission in low excitations species. *Zone B* with a significant scatter in the relations between the line ratios and corresponding to the peak of the  $[\text{OIII}]\lambda 5007$  emission. *Zone C* presenting a behaviour that is a mixture between the two other zones

We have produced statistical frequency distributions of the  $\text{H}\alpha$  radial velocity (Fig. 3, left panel) differentiating pixels from *Zones A* and *B*. The  $[\text{OIII}]\lambda 5007$  histogram shows a single and centred peak in both zones (*A* and *B*). The  $[\text{NII}]\lambda 6584$  presents one redshifted peak in *Zone A* and a bimodal distribution in *Zone B*. This result could be explained as the two components of an expanding and broken shell.

### 3.2 One-dimensional study

Attending to the appearance of each zone at several wavelengths, we selected interesting regions of NGC 6888 to combine fibres producing nine integrated spectra (Fig. 2). Line intensities were measured to obtain physical parameters and chemical abundances (see Table 1). One of the most striking results is the strong enrichment of the N/H that appears enhanced by a factor 6, or even 8 with respect to the solar abundance. Oxygen presents an abundance slightly below the solar value, while helium presents an enrichment too.

To investigate and consolidate both ionization parameter ( $U$ ) and chemical abundances in the different pointings, we performed a grid of photoionization models with the code Cloudy v.8.0. We used one single stellar atmosphere of WN [10] assuming an effective temperature of the star of 50 000 K, with a metallicity of  $Z = 0.008$ . We compared selected emission line ratios of the integrated spectra with models in two diagnostic diagrams (Fig. 3, right panel). Values of  $\log(N/O)$  obtained with the comparison always agree with the abundances calculated with our measurements.

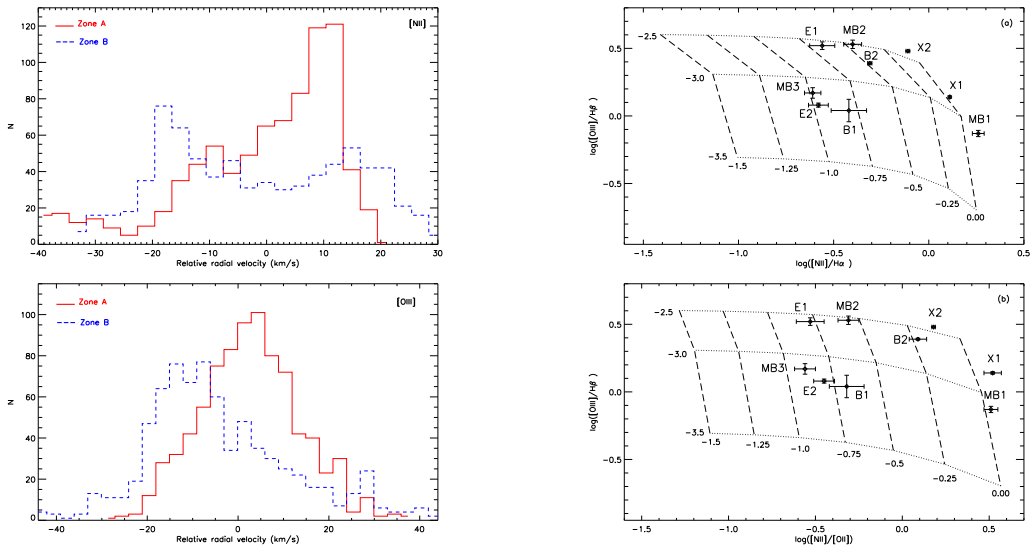


Figure 3: *Left panel:* Statistical frequency distributions of the radial velocity of  $[NII]\lambda 6584$  and  $[OIII]\lambda 5007$ . *Right panel:* Diagnostic diagrams containing the results of our photoionization models (lines) and observed data (points).

## 4 Discussion

We provided a scenario for the evolution of the central WN6 star to explain the features observed in NGC 6888. The proposed scheme consists of a shell structure, but allows irregular and/or broken shells with different physical, kinematical, and chemical properties. (i) An

inner, elliptical, and broken shell, with a strong overabundance in N/H and slightly deficient in O/H. This material corresponds to the red supergiant (RSG) and WR shocked shells. (ii) An outer and spherical shell very bright in oxygen. The helium appears enriched here, while N/H and O/H do not appear enhanced or do not present any slight deficiency. We argue that this shell is the early main-sequence (MS) bubble broken up as a consequence of the collision between RSG and WR shells. (iii) An external and faint shell surrounding the whole nebula like a thin skin. We propose that this shell should represent the early interaction between the bubble created by winds from the MS star with the ISM. The abundances inferred appear to be typical of the local ISM.

## 5 Summary and conclusions

In this proceeding we have summarized the exhaustive study performed over the wind-blown bubble NGC 6888 with integral field spectroscopy [4]. We obtained interpolated images of four regions of the nebula to analyse the ionization structure. In the X-ray emitting zone we generated cubes to carry out a thorough 2D analysis of this region. We generated nine integrated spectra extracted from the four pointings of the nebula measuring line intensities to obtain physical parameters and chemical abundances. We developed a scheme of the internal structure of NGC 6888. It consists of a shell structure (close to “onion-like”) but allowing irregular and/or broken shells. These results agree with the predictions from stellar evolution and nebular formation models.

## References

- [1] Asplund, M., Grevesse, N., Sauval, A. J., & Scott, P. 2009, *ARA&A*, 47, 481
- [2] Bochkarev, N. G. 1988, *Nature*, 332, 518
- [3] Esteban, C. & Vilchez, J. M. 1992, *ApJ*, 390, 536
- [4] Fernández-Martín, A., et al. 2012, *A&A*, 541, A119
- [5] Johnson, H. M. & Hogg, D. E. 1965, *ApJ*, 142, 1033
- [6] Lozinskaya, T. A. 1970, *Soviet Ast.*, 14, 98
- [7] Marston, A. P. & Meaburn, J. 1988, *MNRAS*, 235, 391
- [8] Sánchez, S. F. 2004, *Astronomische Nachrichten*, 325, 167
- [9] Sánchez, S. F. 2006, *Astronomische Nachrichten*, 327, 850
- [10] Smith, L. J., Norris, R. P. F., & Crowther, P. A. 2002, *MNRAS*, 337, 1309
- [11] Wrigge, M., Wendker, H. J., & Wisotzki, L. 1994, *A&A*, 286, 219

Table 1: Electron densities ( $\text{cm}^{-3}$ ), temperatures ( $\times 10^{-4}$  K), ionic abundances, and total chemical abundances for the nine integrated spectra.

	X1	X2	E1	E2	MB1	MB2	MB3	B1	B2	Solar*
$n_e(\text{[SII]})$	179±18	106±16	<100	<100	363±116	<100	<100	105±179	108±26	...
$T_e(\text{[NIII]})$	810±85	9747±108	10171±729	8565±220	7750±72	10199±675	8956±385	8552±412	8537±527	...
$T_e(\text{[OIII]})_E$	6345±98	8416±151	9019±1079	6888±268	5952±79	9061±1003	7371±491	6873±500	6855±639	...
$T_e(\text{[OII]})_E$	7165±185	9016±224	10702±1426	9805±7308	6784±386	11337±6066	9382±6195	7737±1138	7715±1055	...
$T_e(\text{[SII]})_E$	6288±131	7602±159	8798±1012	8161±5189	6017±274	9249±4307	7861±4398	6693±808	6679±749	...
$12+\log(\text{O}^+/\text{H}^+)$	8.09±0.03	7.89±0.02	7.99±0.14	8.22±0.07	8.40±0.04	7.98±0.13	8.24±0.10	8.27±0.13	7.96±0.14	...
$12+\log(\text{O}^{2+}/\text{H}^+)$	8.49±0.03	8.27±0.03	8.20±0.19	8.25±0.08	8.36±0.03	8.20±0.18	8.22±0.13	8.23±0.15	8.57±0.19	...
$12+\log(\text{S}^+/\text{H}^+)$	6.12±0.01	6.04±0.01	6.19±0.08	6.43±0.04	6.54±0.02	6.04±0.08	6.27±0.06	6.43±0.08	5.80±0.08	...
$12+\log(\text{N}^+/\text{H}^+)$	8.17±0.02	7.76±0.02	7.20±0.10	7.37±0.06	8.38±0.02	7.39±0.08	7.31±0.06	7.53±0.08	7.63±0.08	...
$12+\log(\text{Ne}^{2+}/\text{H}^+)$	8.07±0.12	7.87±0.14	...	...	7.83±0.13	...	...	...	8.05±0.24	...
$(\text{He}^+ \lambda 4471/\text{H}^+)$	0.20±0.01	0.19±0.01	0.11±0.02	...	0.16±0.02	...	...	...	0.17±0.02	...
$(\text{He}^+ \lambda 5875/\text{H}^+)$	0.20±0.01	0.22±0.02	0.15±0.04	...	0.16±0.01	0.14±0.02	...	...	0.16±0.01	...
$(\text{He}^+ \lambda 6678/\text{H}^+)$	0.17±0.01	0.17±0.01	...	...	0.14±0.01	...	...	...	0.15±0.01	...
ICF(Ne)	1.09±0.01	1.10±0.01	...	...	1.18±0.02	...	...	...	1.08±0.01	...
$12+\log(\text{O}/\text{H})$	8.64±0.03	8.42±0.02	8.41±0.13	8.54±0.05	8.68±0.03	8.40±0.12	8.53±0.08	8.55±0.10	8.66±0.16	8.69±0.05
$12+\log(\text{N}/\text{H})$	8.72±0.04	8.29±0.04	7.61±0.22	7.68±0.10	8.67±0.05	7.82±0.20	7.60±0.15	7.82±0.18	8.34±0.23	7.83±0.05
$12+\log(\text{Ne}/\text{H})$	8.11±0.12	7.91±0.14	...	...	7.90±0.13	...	...	...	8.08±0.24	7.93±0.10
$\log(\text{N}/\text{O})$	0.08±0.04	-0.13±0.03	-0.79±0.17	-0.85±0.09	-0.01±0.05	-0.58±0.16	-0.93±0.12	-0.74±0.15	-0.32±0.16	-0.86±0.07
$\log(\text{Ne}/\text{O})$	-0.52±0.11	-0.52±0.13	...	...	-0.79±0.12	...	...	...	-0.58±0.07	-0.76±0.11
y	0.17±0.01	0.18±0.01	0.12±0.01	...	0.15±0.01	0.14±0.02	...	...	0.16±0.01	0.09±0.01

$E$  Temperatures derived from other  $T_e$ .

\* Solar values for the total abundances from [1].